Effect of Calcium and Phosphatidic Acid Binding on the C2 Domain of PKCα As Studied by Fourier Transform Infrared Spectroscopy†

Josefa García-García, Senena Corbalán-García, and Juan C. Gómez-Fernández*

Departamento de Bioquímica y Biología Molecular (A), Facultad de Veterinaria, Universidad de Murcia, Apartado de Correos 4021, E-30080 Murcia, Spain

Received March 12, 1999; Revised Manuscript Received May 17, 1999

ABSTRACT: Fourier transform infrared (FTIR) spectroscopy was used to investigate the structural and thermal denaturation of the C2 domain of PKCα (PKC-C2) and its complexes with Ca^{2+} and phosphatidic acid vesicles. The amide I regions in the original spectra of PKC-C2 in the Ca^{2+}-free and Ca^{2+}-bound states are both consistent with a predominantly β-sheet secondary structure below the denaturation temperatures. Spectroscopic studies of the thermal denaturation revealed that for the PKC-C2 domain alone the secondary structure abruptly changed at 50 °C. While in the presence of 2 and 12.5 mM Ca^{2+}, the thermal stability of the protein increased to 60 and 70 °C, respectively. Further studies using a mutant lacking two important amino acids involved in Ca^{2+} binding (PKC-C2D246/248N) demonstrated that these mutations were inherently more stable to thermal denaturation than the wild-type protein. Phosphatidic acid binding to the PKC-C2 domain was characterized, and the lipid−protein binding became Ca^{2+}-independent when 100 mol % phosphatidic acid vesicles were used. The mutant lacking two Ca^{2+} binding sites was also able to bind to phosphatidic acid vesicles. The effect of lipid binding on secondary structure and thermal stability was also studied. β-Sheet was the predominant structure observed in the lipid-bound state, although the percentage represented by this structure in the total area of the amide I band significantly decreased from 60% in the lipid-free state to 47% in the lipid-bound state. This decrease in the β-sheet component of the lipid-bound complex correlates well with the significant increase observed in the 1644 cm^{-1} band which can be assigned to loops and disordered structure. Thermal stability after lipid binding was very high, and no sign of thermal denaturation was observed in the presence of lipids under the conditions that were studied.

Protein kinase C (PKC)[1] is a phospholipid-dependent serine/threonine kinase family consisting of at least 11 closely related isoenzymes. The different PKC isoenzymes play important roles in signal transduction pathways, although the exact significance of each isoenzyme is not known at present. Any elucidation of the regulation mechanism of the various PKC isoenzymes is therefore important (*1*).

Closer examination of protein sequence alignments between PKC isoenzymes reveals blocks of homology between family members, and in every case, these conserved regions have been shown to define protein motifs which confer a specific localization and/or activation input on the isoenzyme (*2*). The module composition allows a more precise categorization of the different PKC subfamilies. There are three main classes of PKC molecules: the classical (α, βI, βII, and γ) that contain the conserved C1 and C2 motifs in the regulatory domain and which are activated by both Ca^{2+}-dependent phospholipid binding and diacylglycerol; the novel (δ, ϵ, η, θ, and μ), which also contain C1 and C2 motifs, although located in reverse order compared to those of the classical isoenzymes, and which are activated by phospholipid and diacylglycerol binding in a Ca^{2+}-independent manner; and finally, the atypical isoenzymes (ζ and ι/λ), whose regulatory domain does not contain any conserved modules and which are not activated by either Ca^{2+} or diacylglycerol (*3*).

C2 domains are sequence motifs that contain approximately 130 amino acids and are present in a large variety of proteins involved in intracellular signaling and membrane trafficking. Crystal structures of C2 domains from synaptotagmin I (*4*), phospholipase C-δ (*5*), phospholipase A2 (*6*), PKCβ (*7*), and PKCδ (*8*) have revealed a highly homologous β-sandwich tertiary fold which serves, in the first four proteins, as the scaffold for a bipartite Ca^{2+} binding site that is formed by a pair of loops which project from the opposing β-sheets. The C2 domains of synaptotagmin and the two phospholipases adopt alternative type I and type II connectivities that differ only by circular permutation of the N and C termini with respect to the tertiary fold (reviewed in refs *9* and *10*). The C2 domains of classical PKCs can be classified as having a type I topology, as demonstrated recently by Sutton and Sprang (*7*). Novel PKCs (PKCδ), on the other hand, exhibit a type II topology similar to that of the phospholipases, although the Ca^{2+} binding site is degenerated (*8*).

† This work was supported by Grants PB95-1022 and PB96-1107 from Direccion General de Enseñanza Superior-MEC (Madrid, Spain) and by Grant 01781/CV/98 from Fundación Séneca (Murcia, Spain).

* Corresponding author. Telephone: +34-968-364766. Fax: +34-968-364147. E-mail: jcgomez@fcu.um.es.

[1] Abbreviations: FT-IR, Fourier transform infrared spectroscopy; PKC, protein kinase C.

10.1021/bi9905765 CCC: $18.00
Published on Web 07/02/1999

The Ca^{2+}-dependent binding of PKC to membranes requires anionic lipids (*11*, *12*). In the absence of diacylglycerol, Ca^{2+} increases the affinity of PKC for anionic phospholipids, which only require a negative charge (*13*). It has been demonstrated both in vivo and in vitro that the C2 domain of PKCα mediates this Ca^{2+}-dependent binding (*14*−*16*). At present, the sequence of events involved in membrane binding and subsequent activation of PKCα is not fully understood.

In this work, we have used FT-IR to study in solution the secondary structure of the PKCα C2 domain during Ca^{2+} and lipid binding independently, and have carried out thermal denaturation studies. Infrared spectra are known to describe directly the secondary structure of the protein backbone (*17*−*19*). The technique is particularly valuable in structural studies of membrane or lipid-associated proteins (*20*−*22*). Our results show that the secondary structure of the C2 domain does not change with Ca^{2+} binding. On the contrary, binding to lipids produces significant conformational changes in the secondary structure of the C2 domain. The thermal denaturation studies revealed that both Ca^{2+} and lipid binding increase the stability of the complexes but by means of different mechanisms.

EXPERIMENTAL PROCEDURES

Construction of Expression Plasmids. The DNA fragment corresponding to the C2 domain of PKCα (residues 158−285) was amplified using PCR with oligonucleotides 5PS and 3PS (sequences CAAGAATTCAAGAGGGGGCGGATTTAC and CAAAAGCTTGTATTCACCCTCCTCTTG, respectively). PKCα cDNA was a kind gift from Drs. Nishizuka and Ono (Kobe University, Kobe, Japan). The resulting 381 bp PCR fragment was subcloned into the *Eco*RI and *Hin*dIII sites of the bacterial expression vectors pGEX-KG (*23*) and pET28c(+), in which the inserts are fused to GST and a six-histidine tag, respectively. Mutations in the C2 domain, which were obtained by substituting aspartic acid at positions 246−248 for asparagine, were generated using PCR mutagenesis (*24*). The resulting DNA fragments which encoded the mutant were subcloned into the same expression vector. All constructs were confirmed by DNA sequencing.

Expression and Purification of the His−PKC-C2 and GST−PKC-C2 Domains. The pET28b(+) plasmid containing the wild-type or mutant PKC-C2 domains was transformed into BL21(DE3) *Escherichia coli* cells. The bacterial cultures (OD_{600} = 0.6) were induced for 5 h at 30 °C with 0.5 mM isopropyl 1-thio-β-D-galactopyranoside (IPTG) (Boehringer Mannheim, Mannheim, Germany). The cells were lysed by sonication in lysis buffer [25 mM Hepes (pH 7.4) and 100 mM NaCl] containing protease inhibitors (10 mM benzamidine, 1 mM PMSF, and 10 μg/mL trypsin inhibitor). The soluble fraction of the lysate was incubated with Ni−NTA agarose (QIAGEN, Hilden, Germany) for 2 h at 4 °C. The Ni beads were washed with lysis buffer containing 20 mM imidazole. The bound fractions were eluted with the same buffer containing 50, 250, and 500 mM imidazole. The six-histidine tag was removed after thrombin cleavage, and finally, the PKC-C2 domain was desalted and concentrated using an Ultrafree-5 centrifugal filter unit (Millipore Inc., Bedford, MA).

The pGEX-KG plasmid containing wild-type or mutant PKC-C2 domains was transformed into HB101 *E. coli* cells. The bacterial cultures (OD_{600} = 0.6) were induced with 0.2 mM isopropyl 1-thio-β-D-galactopyranoside (IPTG) (Boehringer Mannheim) for 5 h at 30 °C. The cells were lysed by sonication in phosphate-buffered saline (PBS) containing protease inhibitors (10 mM benzamidine, 1 mM PMSF, and 10 mg/mL trypsin inhibitor). The soluble fraction of the lysate was incubated with glutathione−Sepharose beads (Pharmacia Biotech, Uppsala, Sweden) for 30 min at 4 °C, which were then washed with PBS three times. Protein concentrations were determined either using the method described by Lowry et al. (*25*) or by densitometry after analyzing the samples on a 15% SDS−PAGE and Coomassie Blue (Sigma, St. Louis, MO) staining.

Preparation of Phospholipids. Lipid vesicles were generated by mixing chloroform solutions of 1-palmitoyl-2-oleoyl-*sn*-glycero-3-phosphocholine (phosphatidylcholine) (Avanti Polar Lipids, Inc., Alabaster, AL) and 1,2-dioleoyl-*sn*-glycero-3-phosphate (phosphatidic acid) (Lipid Product, Nutfield, Surrey, U.K.) at the desired proportions, dried from the organic solvent under a stream of nitrogen, and then further dried under vacuum for 60 min. 1,2-Dipalmitoyl-L-3-phosphatidyl[*N-methyl*-^{3}H]choline (Dupont, Boston, MA; specific activity of 56 Ci/mmol) was included in the lipid mixture as a tracer, at a concentration of approximately 3000−6000 cpm/mg of phospholipid. Dried phospholipids were resuspended in buffer containing 25 mM Hepes (pH 7.4), 0.1 M NaCl, and 0.2 mM EGTA by vigorous vortexing and subjected to direct probe sonication (three cycles of 30 s).

Phospholipid Binding Measurements. (A) A standard assay (*26*) contained 20 μg of the PKC-C2 domain bound to glutathione−Sepharose beads. Beads were prewashed with the respective test solutions and resuspended in 0.1 mL of buffer containing 50 mM Hepes (pH 7.2), 0.1 M NaCl, 0.5 mM EGTA, and 20 μg of the corresponding lipids. The mixture was incubated at room temperature for 15 min with vigorous shaking, and then briefly centrifuged in a tabletop centrifuge. The beads were washed three times with 1 mL of the incubation buffer without liposomes. Liposome binding was then quantified by liquid scintillation counting of the beads.

(B) Gel Filtration Assay. Samples containing 80 μg of the PKC-C2 domain and 320 μg of phospholipids labeled with [^{3}H]phosphatidylcholine were incubated in 100 μL of buffer containing 25 mM Hepes and 0.2 mM EGTA (pH 7.4) for 10 min. The sample was applied on a Sephadex G-100 (Sigma) column (1.0 cm × 2.5 cm) equilibrated and eluted (100 μL/fraction) with the same buffer. The phospholipid elution profile was determined by measuring the radioactivity contained in each fraction. The PKC-C2 domain elution profile was determined by densitometry after using a 15% SDS−polyacrylamide gel and silver staining of each fraction. SDS−polyacrylamide gel electrophoresis was carried out according to Laemmli (*27*) with a 5% stacking and a 15% separating gel. Proteins were detected by silver staining (Bio-Rad, Richmond, CA).

FT-IR Spectroscopy. The lyophilized PKC-C2 domain was dissolved in D_2O at a concentration of approximately 16 mg/mL. The proteins were incubated at 4 °C overnight to maximize H−D exchange. To study infrared amide bands of the proteins in the presence of lipids, small unilamellar vesicles in D_2O buffer containing 25 mM Hepes and 0.2 mM

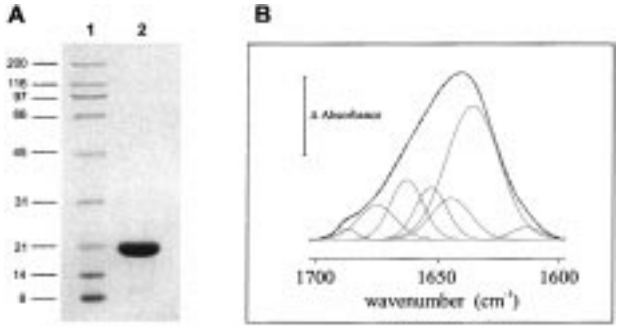

FIGURE 1: (A) SDS−PAGE (15%) showing the PKCα-C2 domain (lane 2). Lane 1 contained molecular mass markers myosin, β-galactosidase, phosphorylase *β*, serum albumin, ovalbumin, carbonic anhydrase, trypsin inhibitor, lysozyme, and aprotinin with masses of 200, 116, 97, 66, 45, 31, 21.5, 14, and 6.5 kDa, respectively. (B) FT-IR spectrum of the PKCα-C2 domain in the amide I region at 25 °C in D_2O buffer (solid line) with the fitted component bands. The position of the individual band was obtained from the resolution-enhanced spectrum. The parameters corresponding to the component bands are reflected in Table 1. The dashed line represents the curve-fitted spectrum. The protein concentration was approximately 16 mg/mL. The increment of absorbance units (△) was 0.05.

EGTA (pD 7.4) were mixed in the desired proportions with the protein solution.

Infrared spectra were recorded using a Philips PU9800 Fourier transform infrared spectrometer equipped with a deuterated triglycine sulfate detector. Samples were examined in a thermostated Specac 20710 cell (Specac, Kent, U.K.) equipped with CaF_2 windows and using 50 μm Teflon spacers. The spectra were recorded after equilibrating the samples at 25 °C for 20 min in the infrared cell. A total of 128 scans were accumulated for each spectrum with a nominal resolution of 2 cm^{-1} and then were Fourier transformed using a triangular apodization function. A sample shuttle accessory was used to obtain the average background and sample spectra. The sample chamber of the spectrometer was continuously purged with dry air to prevent atmospheric water vapor from obscuring the bands of interest. Samples were scanned between 25 and 75 °C at 5 °C intervals with a 5 min delay between each scan using a circulation water bath interfaced to the spectrometer computer. Spectral subtraction was performed interactively using the Spectra-Calc program (Galactic Industries Corp., Salem, NH). The spectra were subjected to deconvolution and second derivation using the same software. Deconvolution was carried out using a γ factor of 2 and a smoothing factor of 0.38. Both deconvolution and derivation gave the number and position, as well as an estimation of the bandwidth and intensity of the bands making up the amide I region. Data treatment and band decomposition of the original amide I have been described previously (*28*, *29*). The fractional areas of the bands in the amide I region were calculated from the final fitted band areas.

RESULTS

FT-IR Studies of the PKC-C2 Domain in D_2O Solution. The C2 domain of rat PKCα (PKC-C2), comprising residues 158−285, was produced using a bacterial expression system as described in Experimental Procedures. The protein was purified to homogeneity by using Ni affinity chromatography (Figure 1A). The protein was separated in a 15% SDS−polyacrylamide gel and then silver stained. Its purity was calculated to be approximately 95%.

The amide I band decomposition of the native PKC-C2 domain in D_2O and 0.2 mM EGTA at 25 °C is shown in Figure 1B. The number and initial position of the component bands were obtained from band-narrowed spectra by Fourier deconvolution and derivation. The corresponding parameters, e.g., band position, percentage area, bandwidth of each spectral component, and assignment, are shown in Table 1. The spectra in D_2O exhibit seven component bands in the 1700−1600 cm^{-1} region, and the quantitative contribution of each band to the total amide I contour was obtained by band curve fitting of the original spectra. The major component in the amide I region appears at 1635 cm^{-1}, and so clearly arises from intramolecular C═O vibrations of *β*-sheets (*18*, *28*−*33*). The high-frequency component at 1675 cm^{-1} can be assigned to the antiparallel *β*-sheet structure (*28*, *34*). Although α-helix usually absorbs at around 1652 cm^{-1}, bands originating from turns, with dihedral angles comparable to those of α-helix, have also been described at this frequency (*29*, *35*, *36*). The band near 1644 cm^{-1} can be attributed to nonstructured conformations, including open loops (*31*, *37*). The bands located at 1663 and 1688 cm^{-1} arise from *β*-turns (*28*, *34*). Additionally, there is a band at about 1612 cm^{-1}, which has been assigned to side chain absorption (*36*−*38*), and so, its contribution is not included in the calculation of the secondary structure of PKC-C2. The secondary structure of the PKC-C2 domain obtained from Table 1 is 60% *β*-sheet (taking account the 1635 and 1675 cm^{-1} bands), 12% α-helix and dihedral turns (similar to α-helix), 15% *β*-turns, and 12% open loops and nonstructured conformation.

Although it has been demonstrated previously that the PKC-C2 domain is involved in Ca^{2+} binding, it is not clear whether this binding affects the conformation of the protein. We studied the effect of Ca^{2+} binding on the secondary structure of the PKC-C2 domain using 2 and 12.5 mM $CaCl_2$, which under the conditions of the assay represent Ca^{2+}:protein ratios of 2:1 and 14:1, respectively. On the basis of the binding assays performed by Nalefski et al. (*39*) for the C2 domain of cytosolic phospholipase A2, the higher concentration would produce maximal binding, while 2 mM is a nonsaturating concentration under the conditions of the FT-IR experiment. The spectra of the protein at 25 °C in the presence of 2 and 12.5 mM $CaCl_2$ both appear to be very similar to that described above for the protein in the absence of $CaCl_2$ (Figure 2), including the number and position of the amide I component bands as indicated in Table 1. There is only a component at 1644 cm^{-1} which exhibits a significant decrease at 12.5 mM $CaCl_2$.

Effect of Ca^{2+} Binding on the Thermal Stability of the PKC-C2 Domain. Further insight into the structural changes that occur during ligand binding was obtained from thermal stability studies. The deconvoluted FT-IR spectra of the PKC-C2 domain in D_2O/EGTA buffer revealed major changes in the amide I mode between 50 and 65 °C (Figure 3A). These changes included a broadening of the overall amide I contour and the appearance of well-defined components at 1615 and 1680 cm^{-1}, which is highly characteristic of thermally denatured proteins (*28*, *40*). These components indicate that extended structures were formed by aggregation of the unfolded proteins, which were produced as a consequence

Table 1: FT-IR Parameters of the Amide I Band Components of the PKC-C2 Domain in D_2O Buffer Containing 25 mM Hepes, 0.2 mM EGTA, and 2 and 12.5 mM Ca^{2+} (pD 7.4)

		25 °C						75 °C		
		0.2 mM EGTA		2 mM Ca^{2+}		12.5 mM Ca^{2+}		0.2 mM EGTA		
position[a] (cm^{-1})	assignment	area[b] (%)	width[c] (cm^{-1})	area (%)	width (cm^{-1})	area (%)	width (cm^{-1})	position (cm^{-1})	area (%)	width (cm^{-1})
1688	β-turns	1	12	2	12	3	13	1680	11	19
1675	antiparallel β-sheet	9	22	8	21	7	17	1670	3	13
1663	β-turns	14	19	14	19	16	18	1663	14	20
1652	α-helix and turns with dihedral angles similar to those of α-helix	12	19	12	19	14	17	1647	34	28
1644	random or open loops	12	24	13	24	9	19	1631	16	22
1635	β-sheet	51	32	50	32	51	31	1615	23	19

[a] Peak position of the amide I band components. [b] Percentage area of the band components of amide I. The areas corresponding to side chain contributions located at 1615−1600 cm^{-1} have not been considered. [c] Half-bandwidth of the amide I components. The values are rounded off to the nearest integer.

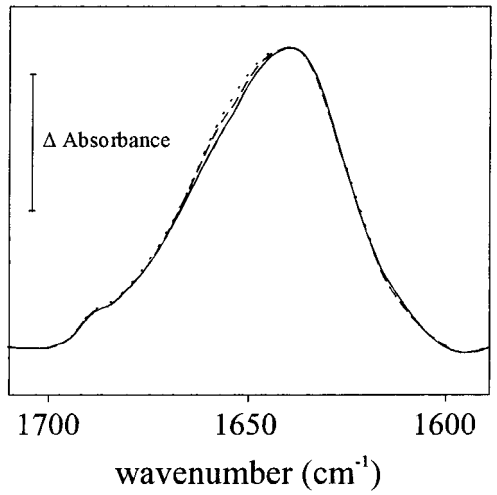

FIGURE 2: FT-IR spectrum of the PKCα-C2 domain in the amide I region at 25 °C in D_2O buffer containing 25 mM Hepes (pD 7.4) and 0.2 mM EGTA (—), 2 mM Ca^{2+} (− − −), or 12.5 mM Ca^{2+} (···). The increment of absorbance units (△) was 0.05.

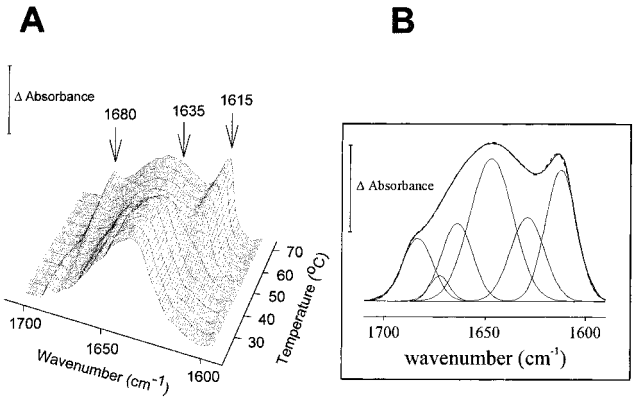

FIGURE 3: (A) Deconvolved FT-IR spectrum of the PKCα-C2 domain in D_2O buffer containing 0.2 mM EGTA in the amide I region (1700−1600 cm^{-1}) as a function of temperature from 25 to 75 °C. Fourier self-deconvolution was carried out using a Lorentzian line shape, a bandwith of 18 cm^{-1}, and a resolution enhancement factor of 2.4. (B) Amide I band decomposition of the thermally denatured PKCα-C2 domain at 75 °C. The increment of absorbance units (△) was 0.05. The parameters corresponding to the component bands are reflected in Table 1.

of irreversible thermal denaturation (*29*, *40*). It is also remarkable to note that apart from the appearance of the 1615 and 1680 cm^{-1} components, other changes in the structure

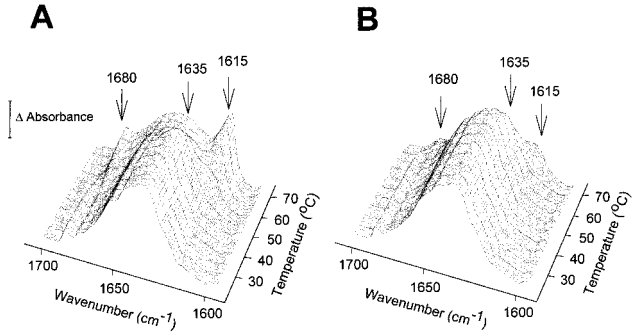

FIGURE 4: Deconvolved FT-IR spectrum of the PKCα-C2 domain in D_2O buffer containing 2 mM Ca^{2+} (A) and 12.5 mM Ca^{2+} (B) in the amide I region (1700−1600 cm^{-1}) as a function of temperature from 25 to 75 °C. The increment of absorbance units (△) was 0.05.

resulted from protein denaturation. The spectrum corresponding to 55−75 °C exhibits a 1647 cm^{-1} band as the major component, which corresponds to an unordered structure and represents 34% of the total area (Table 1). The band at 1631 cm^{-1} corresponds to a β-sheet structure and exhibits two main changes; the percentage of the total area has decreased to 16%, and the maximum wavelength of this component has shifted from 1635 cm^{-1} at 25 °C to 1631 cm^{-1} at 75 °C (Figure 3B). Thus, thermal denaturation of the PKC-C2 domain is characterized by irreversible aggregation and unfolding of the β-sheet structure into a disordered structure.

Figure 4 shows the effect of nonsaturating (2 mM) and saturating (12.5 mM) Ca^{2+} concentrations on the thermal denaturation of the PKC-C2 domain. The addition of 2 mM Ca^{2+} increases the temperature at which thermal denaturation occurs from 55 to 65 °C (Figure 4A), and the final effect was very similar to that obtained in the absence of Ca^{2+} (compare to Figure 3A). However, with 12.5 mM $CaCl_2$ the whole process is shifted to higher temperatures (Figures 4B and 5), indicating that the domain has a higher stability when bound to Ca^{2+}. The half-midpoint temperature of thermal denaturation was calculated to be about 52−53 °C when EGTA was used, 59−60 °C in the presence of 2 mM Ca^{2+}, and >70 °C in the presence of 12.5 mM Ca^{2+} (Figure 5).

To further demonstrate that Ca^{2+} is involved in conferring a higher stability against thermal denaturation to the PKC-C2 domain, we used a construct which contains two

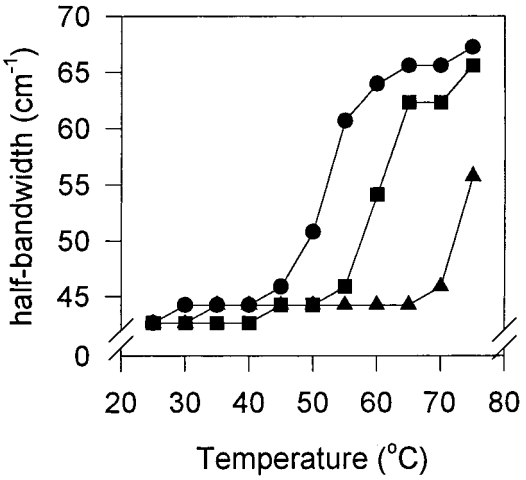

FIGURE 5: Half-bandwidth of the amide I region of the FT-IR spectrum in cm^{-1}, as a function of temperature, for the PKCα-C2 domain in the presence of 0.2 mM EGTA (●), 2 mM Ca^{2+} (■), and 12.5 mM Ca^{2+} (▲).

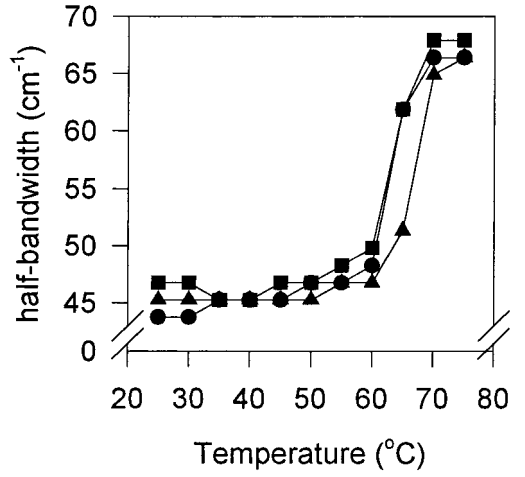

FIGURE 6: Half-bandwidth of the amide I region of the FT-IR spectrum in cm^{-1}, as a function of temperature, for the PKCα-C2D246/248N domain in the presence of 0.2 mM EGTA (●), 2 mM Ca^{2+} (■), and 12.5 mM Ca^{2+} (▲).

mutations from Asp246 and Asp248 to Asn (PKC-C2D246/248N) and which is not able to bind Ca^{2+} (*16*). The FT-IR spectrum at 25 °C was very similar to that of PKC-C2. Thermal denaturation experiments were performed under the same conditions described above for wild-type protein, and as shown in Figure 6, when the mutant was incubated in the presence of EGTA, the denaturation pattern showed higher stability with a transition temperature of 64−65 °C. Maximal denaturation was reached at 70 °C, as with the wild-type PKC-C2 domain. However, when Ca^{2+} was added at concentrations of 2 and 12.5 mM (Figure 6), thermal stability was unaffected, and the transition temperature remained constant at 64−65 °C, suggesting that Ca^{2+} binding is important for stabilization, and demonstrating that Ca^{2+} does not stabilize the protein structure of this mutant as it does the structure of the wild type.

Characterization of Lipid Binding to the PKC-C2 Domain. Several acidic phospholipids have been proposed to be PKC activators, e.g., phosphatidylserine, phosphatidic acid, phosphatidylglycerol, and phosphatidylinositol among others (reviewed in ref *3*). We used small unilamellar vesicles containing phosphatidic acid as a membrane model. Phosphatidylserine was not used in this work because the absorption of its COO^- carboxyl vibration overlaps with the amide I band of the protein, making it very difficult to distinguish between both contributions.

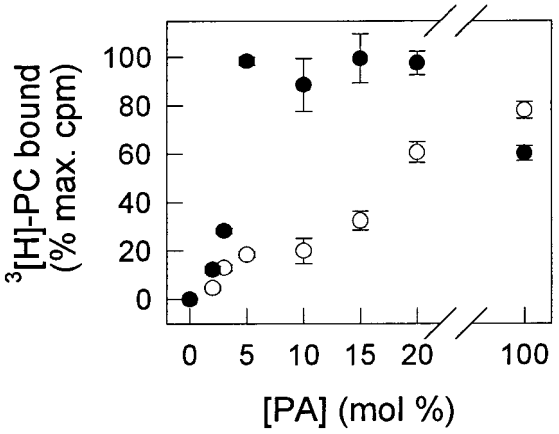

FIGURE 7: Phosphatidic acid-dependent binding of the PKCα-C2 domain. The binding of the PKCα-C2 domain to small unilamelar vesicles containing phosphatidylcholine and increasing mole percentages of phosphatidic acid was measured in the presence of 0.2 mM EGTA (○) and 100 μM free Ca^{2+} (●). Error bars indicate the standard errors of the mean of triplicate determinations.

To characterize the binding of phosphatidic acid vesicles to the PKC-C2 domain, we used an assay where this domain was fused to glutathione *S*-transferase (GST) and purified by affinity chromatography using a glutathione−Sepharose resin. The binding of the PKC-C2 domain to phospholipid vesicles containing [^{3}H]phosphatidylcholine and different proportions of phosphatidic acid (0−100%) was studied in the presence and absence of a saturating Ca^{2+} concentration (100 μM). The binding data showed that 5 mol % phosphatidic acid was required for maximal binding activity when Ca^{2+} was present in the assay (Figure 7). However, the affinity of the domain for lipids decreased in the absence of Ca^{2+}, and became Ca^{2+}-independent when the concentration of phosphatidic acid was increased to 100 mol %. The binding of PKC-C2D246/248N was also tested using vesicles containing 20 and 100 mol % phosphatidic acid. At the lower concentration, this mutant only bound 2.7 ± 0.6% of the maximal binding activity in the absence and 13.3 ± 2.4% in the presence of Ca^{2+}, whereas when 100 mol % phosphatidic acid was used, PKC-C2D246/248N bound to lipid to the same extent as the wild-type protein did.

We used lipid vesicles containing 100 mol % phosphatidic acid as an approximation because this enabled us to study the effect of lipid binding on the PKC-C2 domain in the absence of Ca^{2+}. To confirm that the lipid−PKC-C2 domain bound to phospholipid vesicles under the conditions of our FT-IR experiments, the samples were also examined by gel filtration chromatography using a Sephadex G-100 column. Figure 8 shows a binding assay, where the lipid elution profile was detected from the [^{3}H]phosphatidylcholine contained in each fraction and the PKC-C2 domain profile was determined by densitometry as described in Experimental Procedures. As seen in Figure 8A, the elution profiles of the phosphatidic acid vesicles and PKC-C2 domain overlapped, strongly suggesting that almost 100% of the domain was bound to lipids. In the case of the domain containing the double mutation (PKC-C2D246/248N), the two profiles also overlapped, indicating that most of the protein was also

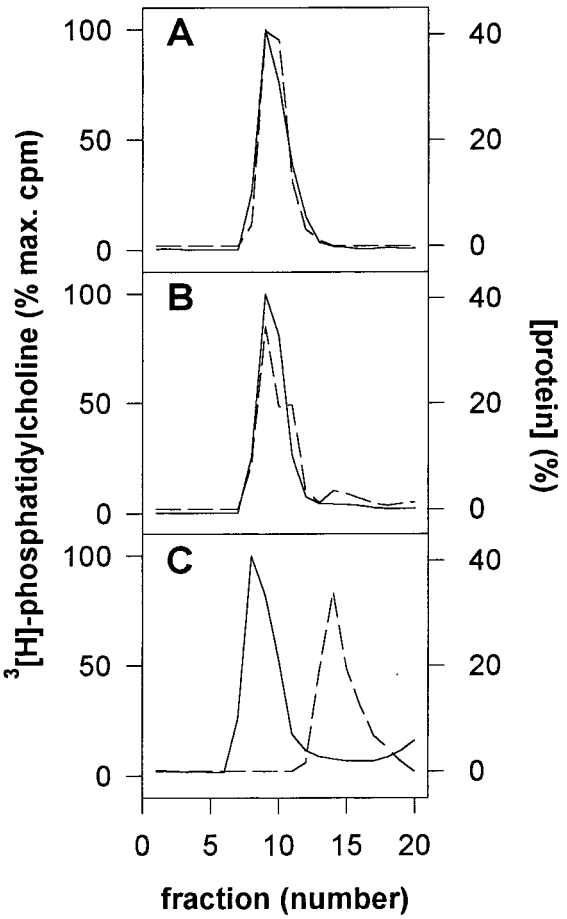

FIGURE 8: Determination of the PKCα-C2 domain binding to phosphatidic acid vesicles by gel filtration using a Sephadex G-100 column. (A) Samples containing 80 μg of the PKC-C2 domain and 320 μg of phosphatidic acid vesicles. (B) Samples containing 80 μg of the PKC-C2D246/248N domain and the same amount of phosphatidic acid vesicles as described above. (C) Samples containing the PKC-C2 domain and 320 μg of phosphatidylcholine. The protein was quantified by densitometry after silver staining.

bound to lipid also (Figure 8B). These results suggest that, although Ca^{2+} increases the affinity of the mutant for membranes, this effect can be suppressed by increased phosphatidic acid concentrations in the membrane. Vesicles containing 100 mol % phosphatidylcholine were used as a nonbinding control, and as demonstrated in Figure 8C, the lipid and PKC-C2 domain peaks did not overlap, indicating that they were not bound.

Effect of Lipid Binding on the PKC-C2 Domain. FT-IR was used to characterize the effect of the PKC-C2 domain's binding to phosphatidic acid on its secondary structure. Figure 9 shows the spectrum and curve fitting obtained from the PKC-C2 domain bound to vesicles containing 100 mol % phosphatidic acid in D_2O at 25 °C in the 1780−1600 cm^{-1} region. The lipid carbonyl-stretching mode is responsible for the absorption observed between 1770 and 1710 cm^{-1}. The curve fitting data suggest a predominance of the β-sheet secondary structure, represented by the 1631 cm^{-1} band. Another important component is the 1644 cm^{-1} band, which was assigned to open loops and nonordered structures. The quantification of the secondary structure of the PKC-C2 domain bound to phosphatidic acid vesicles yielded values of 47% β-sheet, 21% random, 14% α-helix and dihedral turns similar to α-helix, and 17% β-turns (Table 2). It is interesting

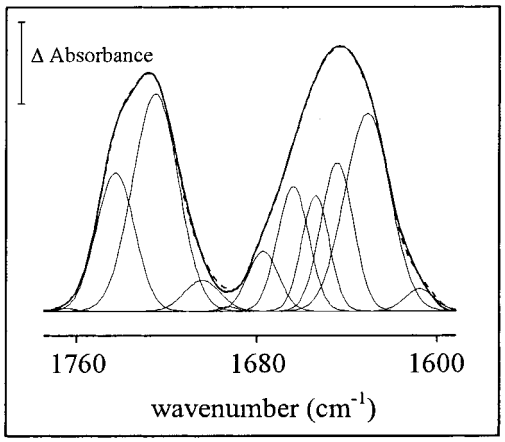

FIGURE 9: FT-IR spectrum of the PKCα-C2 domain in the presence of small unilamelar vesicles containig 100% phosphatidic acid, corresponding to the 1800−1600 cm^{-1} region at 25 °C (—). The parameters corresponding to the component bands are shown in Table 2. The dashed line represents the curve-fitted spectrum. The increment of absorbance units (△) was 0.05.

Table 2: FT-IR Parameters of the Amide I Band Components of the PKC-C2 and PKC-C2D246/248N Domains in the Absence or Presence of Small Unilamellar Vesicles Containing 100 mol % Phosphatidic Acid in 0.2 mM EGTA D_2O Buffer at 25 °C

PKC-C2			PKC-C2D246/248N					
phosphatidic acid			no lipid			phosphatidic acid		
position (cm^{-1})	area (%)	width (cm^{-1})	position (cm^{-1})	area (%)	width (cm^{-1})	position (cm^{-1})	area (%)	width (cm^{-1})
1693	<1	11	1688	3	14	1693	1	14
1677	8	19	1675	7	17	1677	10	22
1663	17	19	1663	17	18	1662	23	22
1653	14	17	1653	11	15	1652	12	16
1644	21	20	1645	9	17	1643	18	19
1631	39	28	1635	53	31	1631	35	29

to note this effect of lipids on the secondary structure of the PKC-C2 domain, especially the decrease in the β-sheet component from 60 to 47% and the increase in the component assigned to random and open loops structure from 12 to 21%.

We have previously demonstrated that the mutant PKC-C2D246/248N binds phosphatidic acid although is not able to bind Ca^{2+}. The percentages of every component obtained after band decomposition of the amide I band of this mutant in the presence of vesicles containing 100 mol % phosphatidic acid are shown in Table 2. As with the wild-type protein, the percentages of the β-sheet and unordered structure components changed, which confirms the binding of the domain to lipid vesicles.

The effect of heating on the structure of PKC-C2 in the presence of phosphatidic acid was also studied by FT-IR (Figure 10A). In the presence of lipid vesicles containing 100 mol % phosphatidic acid, PKC-C2 did not change its FT-IR profile significantly in the temperature range that was tested, suggesting a large increase in stability. As a control, we performed the same assay using PKC-C2 and 100 mol % phosphatidylcholine vesicles, and no binding occurred. In this case, PKC-C2 underwent thermal denaturation with a half-midpoint temperature of 52−53 °C (Figure 10B), exactly the same temperature as in the absence of lipids (see Figure 3A). Figure 10C shows the effect of thermal denaturation on the stability of the PKC-C2D246/248N

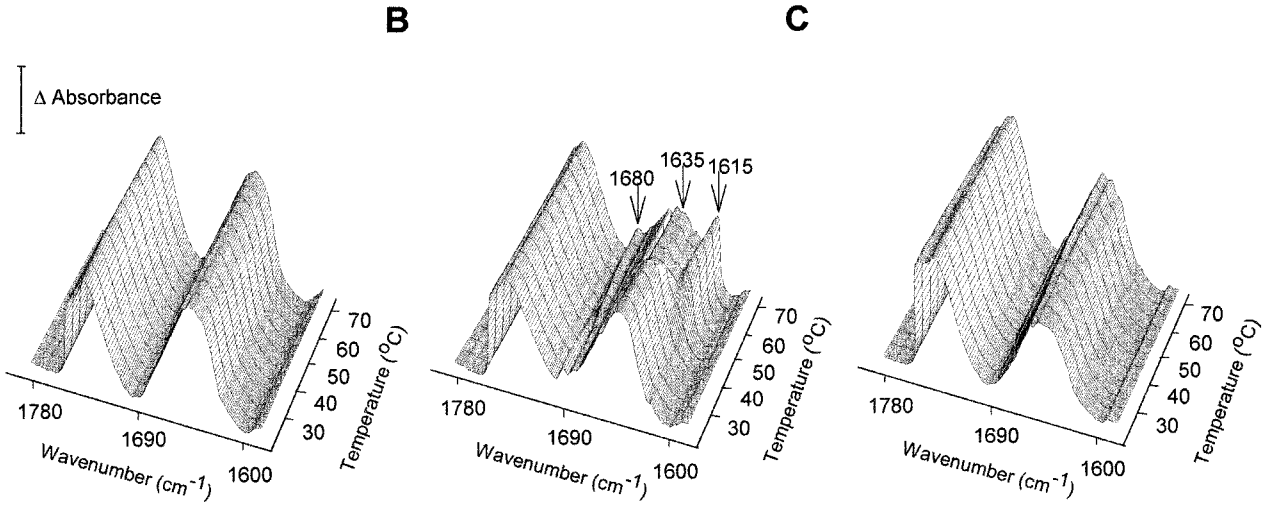

FIGURE 10: Deconvolved FT-IR spectrum of the PKCα-C2 domain in the presence of lipidic vesicles in the 1800−1600 cm^{-1} region obtained at different temperatures. Phosphatidic acid vesicles were incubated with the PKC-C2 domain (A), phosphatidylcholine vesicles and the PKC-C2 domain used as a control (B), and PKC-C2D246/248N (C). The increment of absorbance units (△) was 0.1.

mutant, and as can be appreciated, a big increase in the stability of the protein occurred with lipid binding, confirming that the protein had bound to the lipid vesicles. These data suggest that the amino acidic residues involved in lipid binding are, at least in part, different from those involved in Ca^{2+} binding. Furthermore, lipid interaction led to a very high degree of protein structure stabilization, and no change in secondary structure was detected even after heating to 70 °C.

DISCUSSION

Effect of Ca^{2+} Binding on the PKC-C2 Domain Structure. The aim of this study was to determine the secondary structure of the C2 domain of PKCα in solution and the effect of Ca^{2+} and lipid binding on its structure. X-ray studies of several C2 domains have shown an eight-stranded antiparallel β-sandwich involving 60% of the amino acidic residues (*9*, *10*). These β-sheets are connected by several turns and three loops. Loops 1 and 3 are involved in Ca^{2+} binding in C2 domains of topology I. In particular, the crystal structure of the C2 domain of PKCβ has revealed three Ca^{2+} binding sites. All three sites appear to be hexacoordinate or heptacoordinate, with Ca^{2+}−ligand coordination distances ranging from 2.4 to 2.6 Å. The pseudo-dyad axis of PKCβ-C2 passes through Asp246, which contributes one carboxylate oxygen each to the Ca^{2+} bound to sites 1 and 2. Aspartates 187 and 248 also belong to this pseudo-dyad and are bidentate ligands: Asp187 to Ca^{2+} 1 and Asp248 to Ca^{2+} 2. Aspartates 187 and 248 are also monovalent ligands of Ca^{2+} 2 and Ca^{2+} 1, respectively. Ligands of the third Ca^{2+} ion include Asp254 and Asp248. However, there is some evidence to suggest that this site is only occupied at high Ca^{2+} concentrations in the solution structure of synaptotagmin I (*7*, *41*). Our FT-IR studies on the free-state PKC-C2 domain also show antiparallel β-sheets as the major structure (Figure 1 and Table 1). In the presence of Ca^{2+}, no changes in the secondary structure were observed (Figure 2 and Table 1). These data correlate well with other data previously obtained for the C2 domain of synaptotagmin I, where Ca^{2+} binding only involves rotations of some side chains but causes no substantial backbone rearrangement (*41*, *42*). It is interesting to note that FT-IR detects a band at 1652 cm^{-1} that is usually assigned to α-helix structure. To date, the structures of different C2 domains have not revealed any type of α-helical structure with the exception of the C2 domain of PKCδ (topology type II) that contains a small helix of eight amino acids located between strands β6 and β7. In addition, other authors have demonstrated that bands around 1653 cm^{-1} may result from β-turns that have dihedral angles similar to a turn of the helix (*32*, *35*, *36*). Since the C2 domain of PKCα exhibits type I topology, this component, if it corresponded to an α-helix structure, would constitute an exception within the group exhibiting this topology. Alternatively, and more probably, this component corresponds to turns with a helix-like geometry.

Thus, from the data obtained above, we can conclude that Ca^{2+} does not induce a major change in the secondary structure of the C2 domain of PKCα. However, it is still not clear how Ca^{2+} regulates the C2 domain function. When further information about the effect of Ca^{2+} on the C2 domain was sought using thermal denaturation studies and site-directed mutagenesis, we found that the denaturation mechanism involves irreversible aggregation and unfolding of the scaffold β-sandwich. Ca^{2+} binding stabilized the protein−Ca^{2+} complex during thermal denaturation, and the half-midpoint of denaturation temperature shifted from 50 to 60 °C at 2 mM Ca^{2+} and to approximately 70 °C at 12.5 mM Ca^{2+} (Figure 5). Similar results were obtained by circular dichroism for the C2 domain of synaptotagmin I, where Ca^{2+} binding induced a shift in the denaturation temperature from 55 to 74 °C (*41*).

Studies performed with the PKC-C2D246/248N mutant revealed that these two mutations of Asp246 and Asp248 to Asn are capable of producing by themselves an increase in the domain's stability during thermal denaturation, when the transition temperature shifted from 52 to 64 °C. This temperature shift is very similar to that obtained when a nonsaturating Ca^{2+} concentration was used. When the fact that we only mutated two of the five residues involved in Ca^{2+} binding was considered, these results indicate that neutralization of the negative charges existing in this crevice, either by Ca^{2+} binding or substitution of Asp residues by

Asn, is an important mechanism for stabilizing the protein. Thus, these data confirm that, at least in the case of the C2 domain of PKCα, while Ca^{2+} does not induce a major conformational change, it does produce a structural stabilization that could account for Ca^{2+} regulation, and might modulate the interaction of the domain with acidic lipids.

Effect of Lipid Binding. Several in vitro studies have clearly established that PKC requires anionic lipids for activation (*11*, *12*). Early activity measurements showed that PKC activation specifically required phosphatidylserine (*43*, *44*). However, more recent binding measurements have indicated that, in the absence of diacylglycerol, calcium increases the affinity for anionic phospholipids with no headgroup requirements other than the presence of a negative charge (*13*, *47*, *48*). Therefore, in experiments involving the isolated C2 domain, phosphatidic acid can be used as a legitimate ligand. It should also be noted that, although phosphatidylserine is supposed to be the most specific phospholipid activator for PKC, some authors have claimed that phosphatidic acid may also be an activator of PKC in the absence of Ca^{2+} (*47*, *48*). This is very interesting, since phosphatidic acid acts as a second messenger, which is generated when phospholipase D is activated and might be another signal for the activation of PKC. In this way, PKC isoforms, especially α and βI, have shown to be dowstream targets of PLD (*49*−*51*). More recently, PKCα has been implicated in this pathway in vivo, and such studies have confirmed that phosphatidic acid activates PKCα, in bovine brain cytosol, leading to a Ser/Thr phosphorylation cascade (*52*).

In this study, we have characterized phosphatidic acid binding to the PKC-C2 domain. The results suggest that it has a mechanism very similar to that of phosphatidylserine because at low concentrations its binding to protein depends on Ca^{2+} concentration, but becomes Ca^{2+}-independent when acidic lipid concentration increases. These data suggest that there is an electrostatic component in this interaction and they are also supported by the fact that PKC-C2D246/248N is able to interact with vesicles containing high concentrations of phosphatidic acid (Figure 8). On the contrary, this mutant is not able to bind to vesicles containing a low concentration of phosphatidic acid in a Ca^{2+}-dependent manner. Medkova and Cho (*15*) have recently demonstrated that Arg249 and Arg252 of PKCα (also located in this Ca^{2+} binding crevice) are involved in electrostatic interactions with membranes. In our case, either the PKC-C2 domain or the mutant used still keeps these residues and both bind to high concentrations of acidic lipids, suggesting that the lipid binding site could be located in this area, although it cannot be ruled out that other residues are involved in the lipid binding site.

We have demonstrated that binding to lipids produces a significant change in the secondary structure of the PKC-C2 domain. The percentage of the component corresponding to a β-sheet structure decreases from 60 to 47% of the total amide I band area. This decrease correlates with a significant increase in the 1644 cm^{-1} band (from 12 to 21%) that can be assigned to open loops or disordered structure. Several studies have shown that activation of classical PKCs involves conformational changes, including the removal of the pseudosubstrate region from the active site of PKC (*53*). Thus, ours results suggest that the C2 domain might also be involved in this conformational change during lipid binding which leads to protein activation.

Thermal denaturation studies of PKC-C2−phosphatidic acid complexes reveal the very high stability of the protein compared with its free-Ca^{2+} and Ca^{2+}-bound states, indicating that thermal denaturation does not occur under these conditions, at least in the temperature range studied. This high stability is similar to that described for intrinsic membrane (*54*, *55*).

In summary, the results presented above show that the binding of Ca^{2+} stabilized the secondary structure of the domain against thermal denaturation, that Ca^{2+} and phosphatidic acid interact with different sites of the C2 domain, and that this interaction depends on the density of negative charges on the surface of the phospholipid bilayer. This was demonstrated by the fact that the mutation of the residues involved in the binding of Ca^{2+} did not affect the binding of phosphatidic acid which took place in the absence of Ca^{2+} when the membrane was mainly formed by this phospholipid. This may be taken as an indication that the C2 domain acts simply as an electrostatic switch, as has been claimed for synaptotagmine I (*42*). Nevertheless, on the basis of our results, it is not possible to exclude that subtle changes, which cannot be detected by FT-IR spectroscopy, take place during Ca^{2+} binding and that these changes facilitate the binding of the C2 domain to the lipid membrane. On the other hand, the binding of phosphatidic acid clearly modifies the secondary structure of the domain, and it is tempting to think that this change may affect the activation of PKC. Since the formation of phosphatidic acid by the action of phospholipase D may give rise to local points with high concentrations of this phospholipid, this process might be an alternative way of triggering PKC activation.

When the fact that many signals may generate PKCα activators is taken into account, e.g., the activation of seven-transmembrane and tyrosine kinase receptors or the activation of different phospholipases, a multifunctional C2 domain might allow the protein to respond specifically to each signal, including ways to access different targets. More in vivo work is still necessary to understand this mechanism, although in vitro studies such as that described here also provide important information which will help us to better understand step by step the complete protein kinase C regulation mechanism.

ACKNOWLEDGMENT

We are very grateful to Dr. Ono and Dr. Nishizuka (Kobe University) for the kind gift of the cDNA encoding PKCα.

REFERENCES

1. Hofmann, J. (1997) *FASEB J. 11*, 649−669.
2. Mellor, H., and Parker, P. J. (1998) *Biochem. J. 332*, 281−292.
3. Nishizuka, Y. (1995) *FASEB J. 9*, 484−496.
4. Sutton, R. B., Davletov, B. A., Berghuis, A. M., Südhof, T. C., and Sprang, S. R. (1995) *Cell 80*, 929−938.
5. Essen, L.-O., Perisic, O., Cheung, R., Katan, M., and Williams, R. L. (1996) *Nature 380*, 595−602.
6. Perisic, O., Fong, S., Lynch, D. E., Bycroft, M., and Williams, R. L. (1998) *J. Biol. Chem. 273*, 1596−1604.

7. Sutton, R. B., and Sprang, S. R. (1998) *Structure 6*, 1395−1405.
8. Pappa, H., Murray-Rust, J., Dekker, L. V., Parker, P. J., and McDonald, N. Q. (1998) *Structure 6*, 885−894.
9. Nalefski, E. A., and Falke, J. J. (1996) *Protein Sci. 5*, 2375−2390.
10. Rizo, J., and Südhof, T. C. (1998) *J. Biol. Chem. 273*, 15879−15882.
11. Bazzi, M. D., and Nelsestuen, G. L. (1990) *Biochemistry 29*, 7624−7630.
12. Luo, J. H., Kahn, S., O'Driscoll, K., and Weinstein, I. B. (1993) *J. Biol. Chem. 268*, 3715−3719.
13. Newton, A. C., and Keranen, L. M. (1994) *Biochemistry 33*, 6651−6658.
14. Edwards, A. S., and Newton, A. C. (1997) *Biochemistry 36*, 15615−15623.
15. Medkova, M., and Cho, W. (1998) *J. Biol. Chem. 273*, 17544−17552.
16. Corbalan-Garcia, S., Rodriguez-Alfaro, J. A., and Gomez-Fernandez, J. C. (1999) *Biochem. J. 337*, 513−521.
17. Susi, H. (1969) in *Structure and Stability of Biological Macromolecules* (Timasheff, S. N., and Fasman, G., Eds.) pp 575−663, Marcel Dekker, New York.
18. Krim, S., and Bandekar, J. (1986) *Adv. Protein Chem. 38*, 181−364.
19. Arrondo, J. L. R., Muga, A., Castresana, J., and Goñi, F. M. (1993) *Prog. Biophys. Mol. Biol. 59*, 23−56.
20. Surewicz, W. K., Stepanik, T. M., Szabo, A. G., and Mantsch, H. H. (1988) *J. Biol. Chem. 263*, 786−790.
21. Chapman, D., Jackson, M., and Haris, P. I. (1989) *Biochem. Soc. Trans. 17*, 617−619.
22. Surewicz, W. K., Mantsch, H. H., and Chapman, D. (1993) *Biochemistry 32*, 389−394.
23. Guan, K. L., and Dixon, J. E. (1991) *Anal. Biochem. 192*, 262−267.
24. Saiki, R. K., Gelfan, D. H., Stoffel, S., Scharf, S. J., Higuchi, R., Horn, G. T., Mullis, K. B., and Erlich, H. A. (1988) *Science 239*, 487−491.
25. Lowry, O. H., Rosebrough, N. J., Farr, A. L., and Randall, R. J. (1951) *J. Biol. Chem. 193*, 265−275.
26. Davletov, B. A., and Südhof, T. C. (1993) *J. Biol. Chem. 268*, 26386−26390.
27. Laemmli, U. K. (1970) *Nature 227*, 680−685.
28. Arrondo, J. L. R., Muga, A., Castresana, J., Bernabeu, C., and Goñi, F. M. (1989) *FEBS Lett. 252*, 118−120.
29. Arrondo, J. L. R., Castresana, J., Valpuesta, J. M., and Goñi, F. M. (1994) *Biochemistry 33*, 11650−11655.
30. Susi, H., and Byler, D. M. (1987) *Arch. Biochem. Biophys. 258*, 465−469.
31. Fabian, H., Naumann, D., Misselwitz, R., Ristau, O., Gerlach, D., and Welfle, H. (1992) *Biochemistry 31*, 6532−6538.
32. Gonzalez, M., Bagatolli, L. A., Echabe, I., Arrondo, J. L. R., Argaraña, C. E., Cantor, C. R., and Fidelio, G. D. (1997) *J. Biol. Chem. 272*, 11288−11294.
33. Zhang, H., Ishikawa, Y., Yamamoto, and Carpentier, R. (1998) *FEBS Lett. 426*, 347−351.
34. Muga, A., Arrondo, J. L. R., Bellon, T., Snacho, J., and Bernabeu, C. (1993) *Arch. Biochem. Biophys. 300*, 451−455.
35. Krimm, S., and Bandekar, J. (1992) *Adv. Protein Chem. 38*, 181−364.
36. Bandekar, J. (1992) *Biochim. Biophys. Acta 1120*, 123−143.
37. Susi, H., Timasheff, S. N., and Stevens, L. (1967) *J. Biol. Chem. 242*, 5460−5466.
38. Cladera, J., Galisteo, H. L., Sabes, M., Mateo, P. L., and Padros, E. (1992) *Eur. J. Biochem. 207*, 581−585.
39. Nalefski, E. A., Slazas, M. M., and Falke, J. J. (1997) *Biochemistry 36*, 12011−12018.
40. Surewicz, W. K., Leddy, J. J., and Mantsch, H. H. (1990) *Biochemistry 29*, 8106−8111.
41. Shao, X., Davletov, B. A., Sutton, R. B., Südhof, T. C., and Rizo, J. (1996) *Science 273*, 248−251.
42. Shao, X., Fernandez, Y., Südhof, T. C., and Rizo, J. (1998) *Biochemistry 37*, 16106−16115.
43. Kaibuchi, K., Takai, Y., and Nishizuka, Y. (1985) *J. Biol. Chem. 256*, 7146−7149.
44. Hannum, Y. A., Loomis, C. R., and Bell, R. M. (1986) *J. Biol. Chem. 261*, 7184−7190.
45. Orr, W., and Newton, A. C. (1992) *Biochemistry 31*, 4661−4667.
46. Orr, W., and Newton, A. C. (1992) *Biochemistry 31*, 4667−4673.
47. Epand, R. M., Stafford, A. R., and Lester, D. S. (1992) *Eur. J. Biochem. 208*, 327−332.
48. Senisterra, G. A., van Gorkon, L. C., and Epand, R. M. (1993) *Biochim. Biophys. Res. Commun. 190*, 33−36.
49. Patcher, J. A., Pai, J. K., Mayer-Ezell, R., Petrin, J. M., Dobek, E., and Bishop, W. R. (1992) *J. Biol. Chem. 267*, 9826−9830.
50. Eldar, H., Ben-Av, P., Schmidt, U. S., Livneh, E., and Liscovitch, M. (1993*) J. Biol. Chem. 268*, 12560−12564.
51. Balboa, M. A., Firestein, B. L., Godson, C., Bell, K. S., and Insel, P. A. (1994) *J. Biol. Chem. 269*, 10511−10516.
52. Yokozeki, T., Homma, K., Kuroda, S., Kikkawa, U., Ohno, S., Takahashi, M., Imahori, K., and Kanaho, Y. (1998) *J. Neurochem. 71*, 410−417.
53. Orr, W., Keranen, L. M., and Newton, A. C. (1992) *J. Biol. Chem. 267*, 15263−15266.
54. Corbalan-Garcia, S., Teruel, J. A., Villalain, J., and Gomez-Fernandez, J. C. (1994) *Biochemistry 33*, 8247−8254.
55. Echabe, Y., Dornberger, U., Prado, A., Goñi, F. M., and Arrondo, J. L. R. (1998) *Protein Sci. 7*, 1172−1179.

BI9905765